Biochimica et Biophysica Acta 852 (1986) 106–111
Elsevier

BBA 41940

Interpretation of the polarized electron paramagnetic resonance signal of plant Photosystem I

R.W. Broadhurst [a], A.J. Hoff [b] and P.J. Hore [a]

[a] *Physical Chemistry Laboratory, Oxford University, Oxford OX1 3QZ (U.K.) and* [b] *Department of Biophysics, Huygens Laboratory, State University, Leiden (The Netherlands)*

(Received 9 May 1986)

Key words: ESR; Photosystem I

Attempts to interpret the polarized EPR spectrum of Photosystem I of plant photosynthesis are described. Electron spin polarization is assumed to arise in the primary radical pair P-700$^+$ A_0^- and to be passed to a secondary acceptor A_1 by rapid electron transfer. By including the dipolar interaction between P-700$^+$ and A_0^- and an anisotropic *g*-tensor for A_1^- EPR spectra similar to the experimental lineshape can be simulated. The resulting magnetic parameters are discussed in the light of a recent suggestion that A_1^- may be a semiquinone.

Introduction

Polarized EPR spectra of photoinduced radicals in Photosystem I of plants were first observed by Blankenship et al. [1]. Despite a general understanding of the polarization process [2], clear evidence for the involvement of dipolar interactions between the photoinduced radicals [3,4] and the availability of well-resolved polarized spectra at high microwave frequencies [5,6], no satisfactory interpretation of these signals has yet been proposed.

It is now generally accepted that the EPR polarization phenomenon in photosynthetic reaction centres is caused by the so-called radical pair mechanism [2,7]. According to this mechanism, the parameters that govern the polarized EPR lineshape are the hyperfine interactions, the difference in *g*-values of the geminate radical pair and the magnetic exchange and dipolar interactions between the radicals. In addition, the lineshape is strongly influenced by electron transport from the geminate pair to a third species [8]. The dependence on the intermolecular interactions is perhaps the most interesting aspect of studies on polarized EPR signals, as the dipolar interaction gives information on structure (distance, orientation), whereas the exchange interaction is related to electron-transport rates [9].

Recently we modified Pedersen's theoretical description of the polarized EPR lineshape [8] to include a dipolar interaction between the geminate radicals and so analysed the observed signals from bacterial photosynthetic reaction centres [10]. Here we apply this analysis to the spectrum of Photosystem I reported in Ref. 6. Our premise is that polarization develops in the geminate donor-acceptor pair P-700$^+$ A_0^-, where A_0 is a chlorophyllous species, and is passed from A_0^- to a secondary acceptor, A_1, by electron transport. We show that the observed signal cannot satisfactorily be decomposed into contributions from P-700$^+$ and A_1^- and suggest that part of the signal could

Abbreviations: EPR, electron paramagnetic resonance; RYDMR, reaction yield-detected magnetic resonance.

Correspondence: Dr. P.J. Hore, Physical Chemistry Laboratory, Oxford University, Oxford OX1 3QZ, U.K.

arise from an unpolarized radical that is not directly involved in the charge separation. The remainder of the spectrum is found to be consistent with several combinations of parameters including the orientation of the anisotropic $\boldsymbol{g}$-tensor of A_1^- and the relative strengths of the dipolar and exchange interactions in the geminate pair. The EPR characteristics of A_1^- ($\boldsymbol{g}$-tensor, linewidth) are discussed in the light of a suggestion [6] that this radical may be semiquinone.

Theory

We consider the reaction scheme:

$$\text{P-700}\,A_0A_1 \xrightarrow{h\nu} \text{P-700}^*\,A_0A_1 \rightarrow \text{P-700}^+\,A_0^-A_1 \rightarrow \text{P-700}^+\,A_0A_1^- \tag{1}$$

As in Ref. 10 we assume that spin polarization is generated in $\text{P-700}^+\,A_0^-A_1$ and passed to $\text{P-700}^+\,A_0A_1^-$ by electron transfer and that this step occurs too rapidly to permit EPR detection of the former.

There are contributions to the total polarization arising from the isotropic exchange interaction (J) and the anisotropic dipolar interaction (parameterized by D and E) between P-700^+ and A_0^-. It is assumed that P-700^+ and A_0^- have isotropic, gaussian EPR lineshapes, $L(\text{P})$ and $L(A_0)$, with widths $\Delta B(\text{P})$ and $\Delta B(A_0)$ centred at magnetic fields $B^\circ(\text{P})$ and $B^\circ(A_0)$ which are related to the respective g-values and the microwave frequency, ν, by:

$$B^\circ(\text{P}) = \frac{h\nu}{\mu_B g(\text{P})} \quad \text{and} \quad B^\circ(A_0) = \frac{h\nu}{\mu_B g(A_0)} \tag{2}$$

As before [10], we suppose that A_1^- has an anisotropic EPR spectrum, $L(A_1)$, characterised by principal g-values $g_X(A_1)$, $g_Y(A_1)$ and $g_Z(A_1)$ and gaussian linebroadening, $\Delta B(A_1)$. Under these conditions the polarized EPR spectrum is proportional to (see Ref. 10):

$$J[B^\circ(\text{P}) - B^\circ(A_0)]L(\text{P}) + J[B - B^\circ(\text{P})]L(\text{P})$$

$$+ J[B^\circ(A_0) - B^\circ(\text{P})]\int_0^{2\pi} d\phi \int_0^{\pi} L(A_1)\sin\theta\, d\theta$$

$$+ \frac{D}{6}[B^\circ(A_0) - B^\circ(\text{P})]\int_0^{2\pi} d\phi \int_0^{\pi} L(A_1)(3Z^2 - 1)\sin\theta\, d\theta$$

$$+ \frac{E}{2}[B^\circ(A_0) - B^\circ(\text{P})]$$

$$\times \int_0^{2\pi} d\phi \int_0^{\pi} L(A_1)(X^2 - Y^2)\sin\theta\, d\theta \tag{3}$$

The angles θ and ϕ define the orientation of the principal axes of $\boldsymbol{g}(A_1)$ relative to the magnetic-field direction. The integrals over θ and ϕ represent the spherical averaging necessary for randomly oriented particles. X, Y and Z are given by:

$$X = \sin\alpha\cos\theta\cos(\phi - \beta) - \cos\alpha\sin\theta \tag{4}$$

$$Y = \sin\alpha\sin(\phi - \beta) \tag{5}$$

$$Z = \sin\alpha\sin\theta\cos(\phi - \beta) + \cos\alpha\cos\theta \tag{6}$$

The angles α and β give the direction of the dipolar symmetry axis with respect to the principal axes of $\boldsymbol{g}(A_1)$. The first and second terms in Eqn. 3 represent the P-700^+ subspectrum (net and multiplet effects [2], respectively). The dipolar contribution for P-700^+ disappears in the spherical averaging. The third term is the exchange contribution to the A_1^- subspectrum, while the remaining two terms stem from the dipolar interaction. These do not average to zero because the anisotropy of $\boldsymbol{g}(A_1)$ is correlated with the dipolar anisotropy. A positive (negative) contribution to Eqn. 3 corresponds to an absorptive (emissive) polarization.

In what follows, the theoretical lineshape, calculated from Eqn. 3, is compared with the Q-band (35 GHz) spectrum of Thurnauer and Gast [6].

Methods

Twelve unknown parameters determine the theoretical lineshape: the five g-values $g(\text{P})$, $g(A_0)$, $g_X(A_1)$, $g_Y(A_1)$ and $g_Z(A_1)$; the two linewidths $\Delta B(\text{P})$ and $\Delta B(A_1)$; the angles α and β; the ratios D/J and E/J and a scaling factor. The following strategy was adopted to find the set (or sets) of values of these variables that causes the calculated lineshape to agree most closely with the experimental spectrum.

The experimental spectrum (shown in Fig. 1A, smoothed and integrated to remove the effect of field modulation) consists of five partially re-

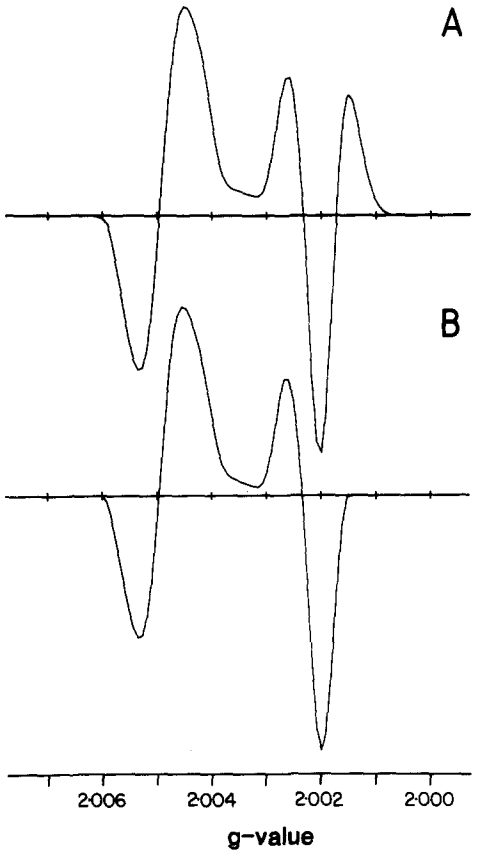

Fig. 1. (A) Smoothed, integrated experimental spectrum of deuterated Photosystem I particles [6]. (B) The experimental spectrum after subtraction of the absorptive peak at $g = 2.0016$. The ordinate is χ'', the imaginary part of the magnetic susceptibility.

solved peaks which we shall label 1 to 5 in order of increasing field (decreasing g-value). The polarizations are, respectively, E, A, A, E and A, with E denoting emission and A absorption. Each of these peaks is first tentatively assigned to one of the two radicals (P-700$^+$ or A_1^-). Using the observed polarizations (E or A) and Eqn. 3, the signs of $[g(P) - g(A_0)]$, D and J and approximate values for α and β are easily deduced. Estimates of the remaining parameters are then found by comparing the experimental spectrum with a few trial-and-error computer simulations. These values are then used as a starting point in an iterative least-squares fit of Eqn. 3 to the experimental lineshape. Holding α and β constant, the remaining parameters (except E/J) are treated as unconstrained variables in a search for minima in the 9-dimensional sum-of-squared-residuals function. The minimization was carried out by means of the 'Spiral' algorithm [11] (a combination of steepest-descent and Gauss–Newton methods) which proved to be both efficient and reliable. Since the algorithm tends to converge to a local minimum close to the starting point, the outcome depends on the initial estimates of the variables and therefore on the proposed assignment. Consequently, several assignments (based on guesswork, intuition and prejudice) were investigated. To cover the (very real) possibility that this subjective approach could miss a promising starting point (and therefore the optimum set of parameter values) grid searches of the 9-dimensional parameter space were also performed. The non-axial dipolar contribution for A_1^- (final term in Eqn. 3) was added on a trial-and-error basis.

To illustrate the first step consider the assignment of peaks 1–3 to A_1^- and 4 and 5 to P-700$^+$. Assuming the P-700$^+$ spectrum consists of an EA multiplet effect superimposed on an E net effect, Eqn. 3 predicts $g(P) > g(A_0)$ and $J > 0$. Similarly for there to be an EAA pattern for A_1^- one must have $D < 0$, $\alpha \approx \pi/2$, $\beta \approx 0$ and $g_X(A_1) > g_Y(A_1)$, $g_Z(A_1)$ (i.e., the P-700$^+$ A_0^- dipolar axis must lie approximately along the X axis of $\boldsymbol{g}(A_1)$).

Results

The strategy outlined above yielded only rather unsatisfactory fits of Eqn. 3 to the experimental spectrum. The main difficulty appears to be that the theoretical lineshape rarely has more than four resolved peaks, whereas the experimental spectrum has five. Several sets of parameters were found for which two of the five peaks were unresolved or one peak entirely missing. The two best simulations are shown in Fig. 2. These were derived from the following assignments: peaks 1–3 to A_1^- and 4 and 5 to P-700$^+$ (Fig. 2A) and peaks 1, 2 and 5 to A_1^- and 3 and 4 to P-700$^+$ (Fig. 2B). Grid searches failed to produce solutions not already found by the assignment method.

The most obvious conclusion is that the theory embodied in Eqn. 3 is inadequate. Although there are several ways in which it could be extended, a

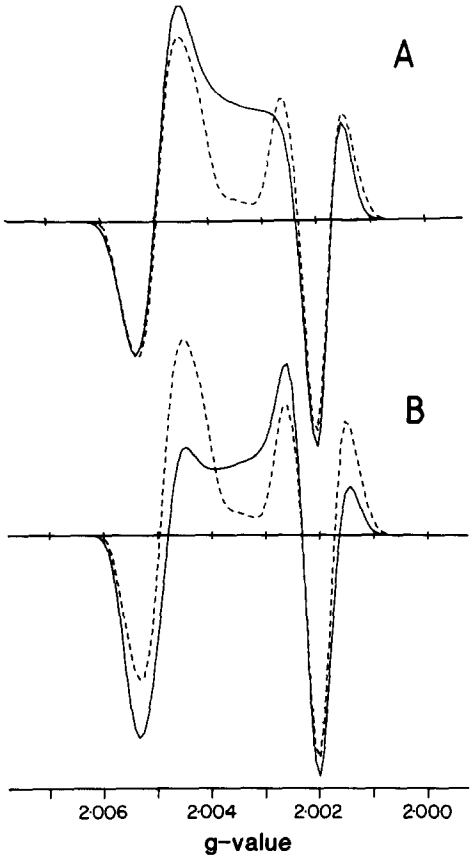

Fig. 2. (A) Solid line: simulated spectrum with $g(P) = 2.00180$, $g(A_0) = 2.00171$, $\Delta B(P) = 2.79G$, $g_X(A_1) = 2.00548$, $g_Y(A_1) = 2.00458$, $g_Z(A_1) = 2.00226$, $\Delta B(A_1) = 2.68G$, $D/J = -41.2$, $E/J = -15.7$, $J > 0$, $\alpha = 90°$, $\beta = 0°$. Dotted line: experimental spectrum. (B) Solid line: simulated spectrum with $g(P) = 2.00218$, $g(A_0) = 2.00234$, $\Delta B(P) = 3.40$ G, $g_X(A_1) = 2.00553$, $g_Y(A_1) = 2.00459$, $g_Z(A_1) = 2.00134$, $\Delta B(A_1) = 2.09G$, $D/J = -27.3$, $E/J = 0$, $J < 0$, $\alpha = 90°$, $\beta = 0°$. Dotted line: experimental spectrum.

simpler way forward is to postulate that only four of the peaks in the spectrum arise from P-700$^+$ and A_1^- and that the fifth is due to another radical. We suggest that the extra resonance is most likely to be peak 5 for the following reasons. If P-700$^+$ is a chlorophyll cation and, as proposed by Thurnauer and Gast [6], A_1^- is a semiquinone, then one would not expect a resonance from either radical to have a g-value as low as ≈ 2.0015. Furthermore, Thurnauer and Gast [6] noted an intensity variation from sample to sample in the high-field region of spectra from photoreduced samples. If a radical other than P-700$^+$ or A_1^- contributes to these spectra, then it might also feature in the time-resolved spectrum discussed here (Fig. 1A).

Accordingly, a peak with absorptive phase, 3.4 G width, centred at $g = 2.0016$ was subtracted from the experimental spectrum to yield the lineshape shown in Fig. 1B. This modified spectrum was subjected to the fitting procedure described above.

In contrast to our experience with the intact spectrum, there is a large number of solutions to this least-squares problem. With the assumption that peaks 3 and 4 arise from P-700$^+$ (as seems most probable) all the acceptable solutions gave $g(P) = 2.0022 \pm 0.0001$, $g(A_0) = 2.0023 \pm 0.0001$, $\Delta B(P) = 3.1 \pm 0.3$G and $J < 0$ for the $E + AE$ pattern. There is less certainty, however, about the parameters for A_1^-. The principal values of the $\boldsymbol{g}$-tensor, the ratio D/J and, to a lesser extent the linewidth, all depend strongly on the initial choice of α and β. It appears that for any pair of angles there is a set of values for $g_X(A_1)$, $g_Y(A_1)$, $g_Z(A_1)$, D/J and $\Delta B(A_1)$ for which Eqn. 3 closely matches the modified experimental spectrum. Thus the orientation of the symmetry axis of the P-700$^+$ A_0^- dipolar interaction relative to the $\boldsymbol{g}$-tensor of A_1^- cannot be determined. Limits can, however, be put on the g-values, the linewidth and D/J. Table I shows the 'best' parameter values when the P-700$^+$ A_0^- dipolar axis is parallel to one of the principal axes of $\boldsymbol{g}(A_1)$. These results and others for intermediate values of α and β indicate that there are two classes of solution:

(i)

$$2.0052 \leqslant g_X(A_1) \leqslant 2.0055$$

$$2.0039 \leqslant g_Y(A_1),\ g_Z(A_1) \leqslant 2.0048$$

$$2.3\ \text{G} \leqslant \Delta B(A_1) \leqslant 4.6\ \text{G}$$

$$\frac{D}{J} \approx \frac{-40}{3\cos^2\psi_X - 1}$$

(ii)

$$2.0050 \leqslant g_X(A_1),\ g_Y(A_1) \leqslant 2.0055$$

$$2.0041 \leqslant g_Z(A_1) \leqslant 2.0042$$

$$2.3\ \text{G} \leqslant \Delta B(A_1) \leqslant 4.6\ \text{G}$$

$$\frac{D}{J} \approx \frac{+40}{3\cos^2\psi_Z - 1}$$

TABLE I

EPR PARAMETERS FROM LINESHAPE SIMULATIONS

Sets of parameter values corresponding to lineshapes matching the modified experimental spectrum, Fig. 1B. Orientations X, Y and Z correspond to $\alpha = \pi/2$ and $\beta = 0$, $\alpha = \pi/2$ and $\beta = \pi/2$, and $\alpha = 0$, respectively. The dipolar interaction was assumed to be axial for these simulations, i.e., $E = 0$.

	X	Y	Z	X	Y	Z
$g(P)$	2.00220	2.00218	2.00216	2.00218	2.00217	2.00218
$g(A_0)$	2.00233	2.00230	2.00233	2.00233	2.00233	2.00235
$\Delta B(P)/G$	3.17	3.04	3.01	3.11	3.07	3.43
$g_X(A_1)$	2.00545	2.00532	2.00523	2.00524	2.00523	2.00523
$g_Y(A_1)$	2.00466	2.00444	2.00474	2.00507	2.00524	2.00520
$g_Z(A_1)$	2.00397	2.00445	2.00445	2.00414	2.00418	2.00415
$\Delta B(A_1)$	2.48	4.09	4.62	3.74	3.46	3.82
D/J	−18.9	+48.1	+40.2	−38.0	−41.4	+20.6

where ψ_X (ψ_Z) is the angle between the X (Z) axis of $\boldsymbol{g}(A_1)$ and the dipolar axis of P-700$^+$ A_0^- and is a function of α and β. On the grounds of goodness-of-fit there is no reason to prefer one class of solution over the other.

A representative theoretical lineshape is shown in Fig. 3. Note that peaks 1 and 2 arise from A_1^-, while 3 and 4 are from P-700$^+$.

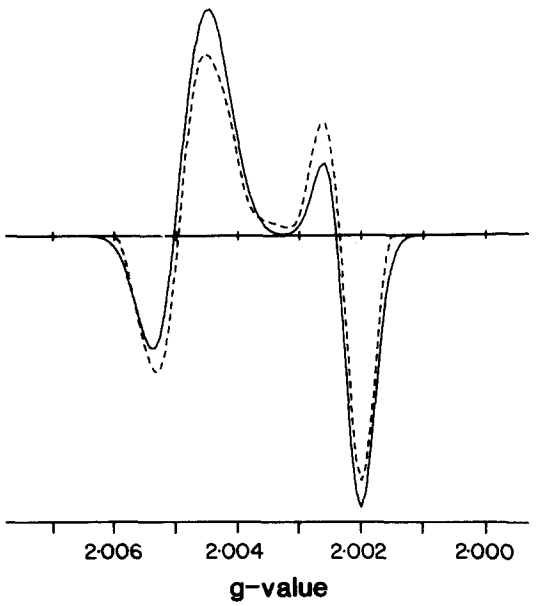

Fig. 3. Solid line: simulated spectrum with $g(P) = 2.00218$, $g(A_0) = 2.00233$, $\Delta B(P) = 3.11$ G, $g_X(A_1) = 2.00524$, $g_Y(A_1) = 2.00507$, $g_Z(A_1) = 2.00414$, $\Delta B(A_1) = 3.74$G, $D/J = -38.0$, $E/J = 0$, $J < 0$, $\alpha = 90°$, $\beta = 0°$. Dotted line: experimental spectrum after subtraction of the high-field peak.

Discussion

The results just described may be summarized as follows. On the one hand we obtain a rather poor quality agreement between the intact experimental spectrum and the theoretical lineshape (Fig. 2A and B), and on the other hand a rather good agreement (e.g., Fig. 3) with the spectrum modified in a way that is difficult to justify. Neither outcome is particularly satisfactory.

The simulation shown in Fig. 2A is attractive in that the $\boldsymbol{g}$-tensor components for A_1^- are close to those found for the analogous acceptor (ubisemiquinone) in bacterial reaction centres [12]. Similar principal values have been found by Thurnauer and Gast [6] for a stable reduced species, presumably a mixture of A_0^- and A_1^-, with a significant component near 2.0026 due to A_0^-. Optical measurements [13] show that reduction of A_1 is not accompanied by absorption changes in the visible, supporting its identification with a quinone species. Furthermore, this simulation requires the dipolar parameter D to be negative in agreement with the interpretation of RYDMR (reaction yield detected magnetic resonance) spectra of *Rhodobacter sphaeroides* (formerly called *Rhodopseudomonas sphaeroides*) [14]. Although a negative value for the exchange parameter would be expected for a radical pair, J may become positive (as needed for the $E + EA$ pattern of peaks 4 and 5) if superexchange interactions with an intercalated molecule are important [15].

The other simulation of the intact spectrum,

Fig. 2B, suggests that one of the **g**-tensor components of A_1^- is as low as 2.00134 to account for the high field absorptive peak. Such a value militates against the identification of A_1^- as a semiquinone. Moreover, the positive sign of D is problematical.

The spectrum remaining after subtraction of peak 5 appears to be consistent with a number of sets of parameters, falling into two classes. These agree in predicting an approx. axial **g**-tensor for A_1^- and differ in the direction of the anisotropy (i.e., $g_X(A_1) > g_Y(A_1) \approx g_Z(A_1)$ or $g_X(A_1) \approx g_Y(A_1) > g_Z(A_1)$). Neither corresponds particularly closely to the **g**-tensor components expected for a semiquinone. If the subtracted signal at $g = 2.0016$ is not due to P-700$^+$ or A_1^-, then its origin is unknown. One may speculate that P-700$^+$ has some interaction with a photooxidised neighbouring chlorophyll, giving rise to exchange splitting in some of the reaction centres.

All the simulations, however, are in reasonable agreement about the g-values of P-700$^+$ and A_0^- (2.0017–2.0023). Though perhaps a little low for chlorophyllous species (cf. 2.0026 for P^+ in bacteria [16]), such values are not too surprising. More unusual, however, are the large $|D/J|$ ratios. This quantity seems to be less than 3 for quinone-depleted bacterial reaction centres (reviewed in Ref. 17). The large value found here may indicate that P-700$^+$ and A_0^- are considerably further apart than the corresponding molecules in bacterial reaction centres (J decreases more rapidly with separation than does D). Also, it is possible that anisotropic contributions to the hyperfine interactions of P-700$^+$ may lead to smaller D/J ratio without substantially affecting the EPR lineshape (Hore, P.J. and Broadhurst, R.W., unpublished results). Interestingly, our interpretation of the polarized EPR spectra of bacteria in which the quinone is still present also suggested a large ratio of D to J [10].

In conclusion, it has not proved possible to find an entirely satisfactory interpretation of the polarized EPR spectrum of Photosystem I. The ambiguities noted here can be resolved by studying electron spin polarization of oriented Photosystem I particles at high microwave frequencies, and we expect future work to concentrate on such experiments.

References

1 Blankenship, R., McGuire, A. and Sauer, K. (1975) Proc. Natl. Acad. Sci. USA 72, 4943–4947
2 Hoff, A.J. (1984) Q. Rev. Biophys. 17, 153–282
3 McCracken, J.L, Frank, H.A. and Sauer, K. (1982) Biochim. Biophys. Acta 679, 156–168
4 McCracken, J.L. and Sauer, K. (1983) Biochim. Biophys. Acta 724, 83–93
5 Furrer, R. and Thurnauer, M.C. (1983) FEBS Lett. 153, 399–403
6 Thurnauer, M.C. and Gast, P. (1985) Photobiochem. Photobiophys. 9, 29–38
7 Kaptein, R. and Oosterhoff, L.J. (1969) Chem. Phys. Lett. 4, 195–197
8 Pedersen, J.B. (1979) FEBS Lett. 97, 305–310
9 Hopfield, J.J. (1976) in Electrical Phenomena at the Biological Membrane Level (Roux, E., ed.), pp. 471–492, Elsevier, Amsterdam
10 Hore, P.J., Watson, E.T., Pedersen, J.B. and Hoff, A.J. (1986) Biochim. Biophys. Acta 849, 70–76
11 Jones, A. (1970) Computer J. 13, 301–308
12 Gast, P., Swarthoff, T., Ebskamp, F.C.R. and Hoff, A.J. (1983) Biochim. Biophys. Acta 722, 163–175
13 Mansfield, R.W. and Evans, M.C.W. (1985) FEBS Lett. 190, 237–241
14 Norris, J.R., Bowman, M.K., Budil, D.E., Tang, J., Wraight, C.A. and Closs, G.L. (1982) Proc. Natl. Acad. Sci. USA 79, 5532–5536
15 Hoff, A.J. and Hore, P.J. (1984) Chem. Phys. Lett. 108, 104–110
16 Hoff, A.J. (1982) Biophys. Struct. Mech. 8, 107–150
17 Hoff, A.J. (1986) Photochem. Photobiol., in the press